Blue Multifocal Pupillographic Objective Perimetry in Glaucoma

Corinne F. Carle,[1] Andrew C. James,[1] Maria Kolic,[1] Rohan W. Essex,[1,2] and Ted Maddess[1]

[1]John Curtin School of Medical Research, The Australian National University, Canberra, Australia
[2]Department of Ophthalmology, The Canberra Hospital, Canberra, Australia

Correspondence: Corinne F. Carle, John Curtin School of Medical Research, The Australian National University, GPO Box 334, Canberra City, ACT 2600, Australia; corinne.carle@anu.edu.au.

Submitted: November 7, 2014
Accepted: August 17, 2015

Citation: Carle CF, James AC, Kolic M, Essex RW, Maddess T. Blue multifocal pupillographic objective perimetry in glaucoma. *Invest Ophthalmol Vis Sci.* 2015;56:6394–6403. DOI:10.1167/iovs.14-16029

Purpose. This study investigated multifocal pupillographic objective perimetry (mfPOP) stimuli that target the intrinsic photosensitivity of melanopsin retinal ganglion cells. The diagnostic potential for glaucoma is compared between stimuli biased toward either cone input to these cells or their melanopsin response.

Methods. Nineteen glaucoma patients and 24 normal subjects were tested using mfPOP stimulus protocols with either 33-ms yellow or 750-ms blue stimuli. Subjects' color discrimination was assessed using the Farnsworth 100-hue test. Pupillary responses were measured, and mixed-effects regression was used to quantify results. Diagnostic accuracy was assessed using receiver operating characteristic (ROC) analysis.

Results. The mean reduction in moderate to severe glaucoma pupil responses using blue mfPOP stimuli was larger but more variable than that of the shorter yellow stimuli (blue: −1.32 dB [$t(40) = -2.29$; $P = 0.027$]; yellow: −0.93 dB [$t(40) = -3.13$; $P = 0.003$]). Color discrimination decreased significantly with age and glaucoma, with type III blue-yellow anomalies dominating. ROC analysis revealed similar diagnostic accuracies (AUC for eyes classified as moderate to severe; blue: 81.7%, yellow: 83.7). Slightly higher sensitivity and specificity were obtained using blue stimuli in mild disease (AUCs blue: 71.1, cf. yellow: 67.7), although this difference was not significant.

Conclusions. In moderate to severe glaucoma, diagnostic accuracy of yellow and blue was similar, but blue stimuli showed limited ability to resolve scotomas. Blue mfPOP stimuli, however, may have advantages over yellow in detecting early glaucoma.

Keywords: glaucoma, melanopsin, pupil, visual field

Accurate, fast, and objective measurement of visual fields is critical to the assessment of disorders such as glaucoma. With this goal in mind, various forms of pupillographic perimetry have been attempted,[1–3] some using multifocal methods.[4,5] We have designed multifocal pupil stimuli that are both temporally and spatially sparse, based on techniques originally developed for evoked potentials.[6–8] This method, known as multifocal pupillographic objective perimetry (mfPOP), allows us to measure the mean amplitude of pupil constrictions in response to numerous stimulus presentations made in each of 44 visual field test-regions per eye. Our recent mfPOP studies have produced promising results in detection of glaucoma and other diseases[9–16] and have taught us much about the pupillary system.[17–19]

Increasing knowledge of the involvement of intrinsically photosensitive retinal ganglion cells (ipRGCs) in pupillary responses has encouraged development of novel color-variant pupillographic methods. Outer retinal input to ipRGCs comprises "ON" luminance signal from medium-wavelength–sensitive (M-) and long-wavelength–sensitive (L-) cone photoreceptors and, at lower luminances, rod photoreceptors; and "OFF" signal from short-wavelength–sensitive (S-) cones.[20,21] In addition, ipRGCs possess an intrinsic response due to the photopigment melanopsin.[22–24] This intrinsic component has a peak sensitivity of 482 nm and has much slower response dynamics than cone-driven responses.[25,26] Techniques developed initially by Kardon et al.[25] and Park et al.[27] use these characteristics to preferentially target inner (rod/cone) or outer (RGC) functions using red or blue full-field stimuli of suitable intensities.

Application of these full-field methods in glaucoma has relied largely on the measurement of the postillumination pupil response (PIPR) to dark-adapted central-field stimulation.[28,29] This sustained response component, which occurs following the peak of constrictions, is attributed largely to melanopsin, because its spectral sensitivity and temporal characteristics closely match those of ipRGCs' intrinsic response.[25,26] McDougal and Gamlin[26] showed that once this melanopsin response is activated, shunting of outer retinal signal produces "winner-takes-all" behavior in the intrinsic response of these cells. Responses to stimuli bright enough to result in a pupil diameter of approximately 3 mm were found to be dominated by melanopsin; for short duration stimuli, these measurements incorporated early response components including the peak of the response.[26] This means that under conditions which elicit a low-level but continuous melanopsin response such as our mfPOP protocols, the peak amplitudes of constrictions due to light increments from this baseline level are also likely dominated by melanopsin. It seems plausible therefore, by presenting blue stimuli on a photopic background, to use mfPOP to elicit responses with a substantial melanopsin

Table 1. Subject Group Characteristics, Plus Temporal and Luminance Characteristics of the Stimulus Protocols for the Main and Preliminary Experiments

Stimulus Characteristics	Preliminary Experiment								Main Experiment	
Subjects, *n*, mean ± SD age, y	Normal: 4 (2 males), 48.3 ± 10.4								Glaucoma: 19 (10 males), 64.1 ± 9.8 Normal: 24 (10 males), 59.8 ± 7.3 y	
Color	Blue	Blue	Blue	Blue	Red	Red	Red	Red	Blue	Yellow
Luminance, cd/m^2	45	55	65	75*	45	55	65	75	75*	150†
Duration, ms	750	750	750	750	750	750	750	750	750	33
Mean interval between presentations/region, s	32	32	32	32	32	32	32	32	32	4
Average number of stimuli shown in each test-region	15	15	15	15	15	15	15	15	15	60
Recording duration, min	8	8	8	8	8	8	8	8	8	4

Experimental protocols differed in color, stimulus luminance and duration, presentation rate, and recording duration. Stimuli were presented on a photopic background the same color as the stimuli but with a mean luminance of 10 cd/m^2 (Fig. 1B). For details of the stimulus spectra, CIE coordinates and relative cone activations refer to Figures 1D, 1E, 1F.

* Protocols are identical.

† Luminance values ranged between 67 and 150 cd/m^2 depending on visual field location (Fig. 1C).

component and enable topographic assessment of the intrinsic ipRGC response.

The mfPOP test protocols currently under development use yellow stimuli,[10,12] which minimizes any confounding effects of lens brunescence[30–33] or variations in macular pigment density.[34,35] These transient (33-ms) yellow stimuli favor the excitatory extrinsic input of M- and L-cones to ipRGCs[12]; M- and L-cones also contribute to pupillary responses via cortical projections to the pretectum originating in midget and parasol ganglion cells.[10,36–38] The targeting of ipRGCs through their intrinsic melanopsin response and minimization of midget and parasol ganglion cell involvement, however, may confer benefits in glaucoma assessment due to the sparse distribution and limited spatial redundancy of these melanopsin-containing cells.[39] This study therefore compares the response characteristics and diagnostic utility for glaucoma of a yellow stimulus protocol using transient stimuli, with a protocol using blue stimuli of long duration designed to target the intrinsic component of the ipRGC response.

Methods

This study consisted of two parts. The first part was a preliminary experiment to assess the characteristics of pupil responses to 750-ms red and blue mfPOP stimuli at four luminance levels, to determine whether the results for blue stimuli matched expectations from published studies for melanopsin-driven responses. The main experiment compared responses to 750-ms blue mfPOP stimuli with responses to our standard 33-ms yellow in glaucomatous and normal eyes.

Subjects

Four normal subjects participated in the preliminary experiment (Table 1). Their visual acuity was checked and visual fields assessed using Humphrey FDT C-20 full threshold perimetry (Carl Zeiss Meditec, Inc., Dublin, CA, USA). Exclusion criteria are outlined below.

In the main experiment, 43 subjects were tested with blue and yellow variants of mfPOP. Diagnostic status was confirmed using Humphrey (HFA II) achromatic SITA-fast perimetry, Matrix 24-2 perimetry, and Stratus OCT (all from Carl Zeiss Meditec, Inc.), fundus photography, slit-lamp biomicroscopy, and applanation tonometry. Color vision was assessed using the Farnsworth 100-hue test (F100; Luneau Ophthalmologie, Chartres, France). One putatively normal subject's data were excluded from analysis due to a F100 result exceeding the 95th percentile of published norms.[40] Final study group characteristics are shown in Table 1 and Supplementary Table S1. Both eyes of each subject were tested concurrently ($n = 86$ visual fields). Informed written consent was given by all participants after the nature and possible consequences of the study were explained, under ANU Human Experimentation Ethics Committee approval 238/04. All research adhered to the tenets of the Declaration of Helsinki.

Glaucoma subjects were recruited from the Canberra Eye Hospital and were required to have a diagnosis of open-angle glaucoma with evidence of glaucomatous scotomas in at least one eye (four subjects had normotensive glaucoma). Eyes of glaucoma subjects were classified based on HFA mean deviation (MD) as follows: moderate to severe glaucoma was defined as MD less than –6 dB (13 eyes); mild glaucoma as MD equal to or greater than –6 dB (22 eyes); and ND denoted no apparent field defects (3 fellow eyes). Normal subjects, recruited from local optometric practices or by word of mouth, were required to have no detectable glaucomatous abnormalities, open angles, discs within normal limits, and intraocular pressure of <21 mm Hg. Clinical characteristics of subjects are provided in Supplementary Table S1.

Exclusion criteria for all subjects in both experiments included evidence of other ocular pathology or previous ocular surgery (argon or selective laser trabeculoplasty excepted in patients), refractive errors greater than ±6 diopters or more than 2 diopters of cylinder, or systemic disease or medication that might impair vision or pupillary responses. Subjects were requested to not consume caffeine or alcohol for 1 hour before testing.

Multifocal Infrared Pupillography

Presentation of mfPOP stimuli and monitoring of pupil diameter were carried out using a prototype of the US Food and Drug Administration–approved nuCoria Field Analyzer (nuCoria Pty. Ltd., Acton, Australia). This tabletop device uses concurrent, dichoptic presentation of temporally and spatially sparse multifocal stimuli at 60 frames/s.[9,11,12] Infrared light was used to illuminate subjects' pupils and their responses were monitored by separate video cameras at 30 frames/s/eye. During testing, subjects fixated on a small cross in the center of the viewing field. Stimuli were presented at optical infinity to minimize accommodative responses. Binocular fusion of the two images was aided by large crosshairs and the low-contrast (less than ±0.1) radial sinusoidal variation of the stimulus background (Fig. 1B). Gaze was monitored online, and data from

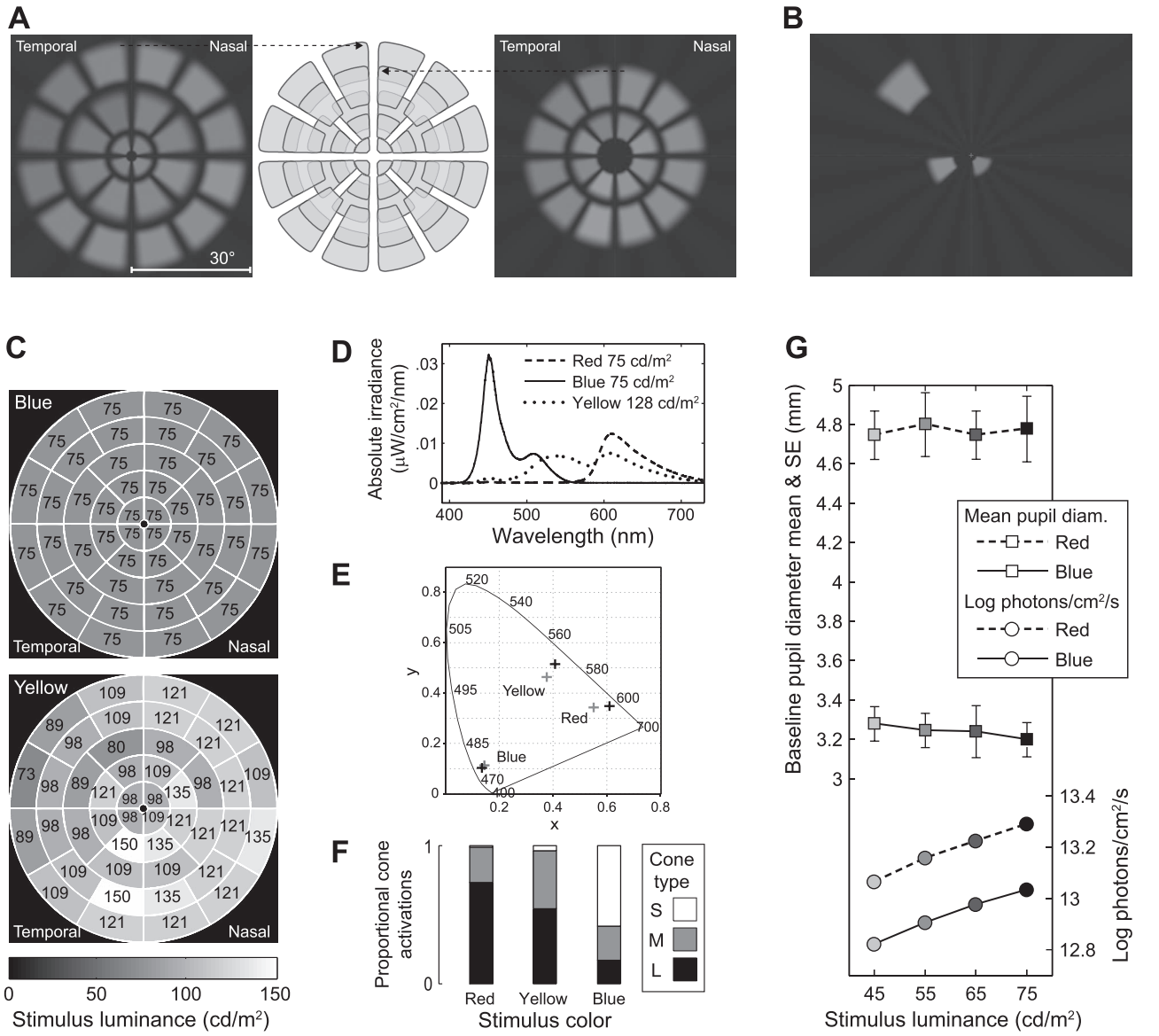

Figure 1. Stimulus color and luminance characteristics. (**A**) Left-eye–equivalent test-region map for the luminance-balanced yellow stimulus protocol of the main experiment (shown in *grayscale*). The outer, median, and central rings of regions are shown at *left*, intermediate rings at *right*. These two maps, overlaid in the manner shown at *center*, result in a 44-region-per-eye layout. This left-equivalent map was inverted left-to-right for the right eye so that any temporonasal variations in luminance were maintained. (**B**) A single frame of the yellow stimulus protocol as viewed by a subject (shown in *grayscale*). The radial background for each protocol was the same color as the stimulus in each case but was displayed at a lower mean luminance of 10 cd/m^2. Temporal and spatial sparseness of the stimulus presentation is apparent in the small proportion and diffuse spacing of the test-regions active in this frame. The dichoptic presentation of these stimuli means that some of these regions are viewed by one eye and the remainder by the other eye, in a cyclopean view. Thus, the two separate images are fused by the subject to form the percept shown. (**C**) Test-region luminances for the protocols of the main experiment. The yellow protocol used luminance-balanced stimuli, and therefore luminances varied among regions (Maddess T, et al. *IOVS* 2009;50:ARVO E-Abstract 5281; Kolic M, et al. *IOVS* 2009;50:ARVO E-Abstract 5280). This subtle variation can be seen in (**A**); compare the luminance of the brightest region in the inner ring of the *right-hand* figure (150 cd/m^2) with that of the dimmest region immediately *above* the midline at the far left of the *left-hand* figure (67 cd/m^2). All other protocols used stimuli presented at a single luminance level, as in the 75 cd/m^2 test-regions of the blue protocol shown here. (**D**) Color spectra for each of the stimuli. (**E**) CIE coordinates with test-region values plotted in *black* and backgrounds in *gray*. (**F**) Proportional cone activations for the stimuli. (**G**) Mean baseline pupil diameters across all subjects (*filled squares*) for the protocols used in the preliminary experiment and log photon/cm^2/s equivalents (*filled circles*) for each stimulus luminance and color. Note that the 75 cd/m^2 blue condition is the same as that used in the main experiment. Values for these are reported in Supplementary Table S2.

blinks and fixation losses were deleted. The mfPOP method can tolerate up to 15% data loss before a given 30-second segment must be repeated. Corrective lenses compensated for refractive errors to within 1.5 diopters; the stimuli contained no spatial frequencies above 2 cyc/deg, making them tolerant of this degree of misrefraction.[41]

Stimuli

The stimulus layout used in both experiments extended ±30° from fixation and consisted of 44 visual field test-regions arranged in an overlapping dartboard configuration (Fig. 1A).[11] The two experimental conditions (stimulus protocols) of the main experiment used either transient 33-ms stimuli consisting

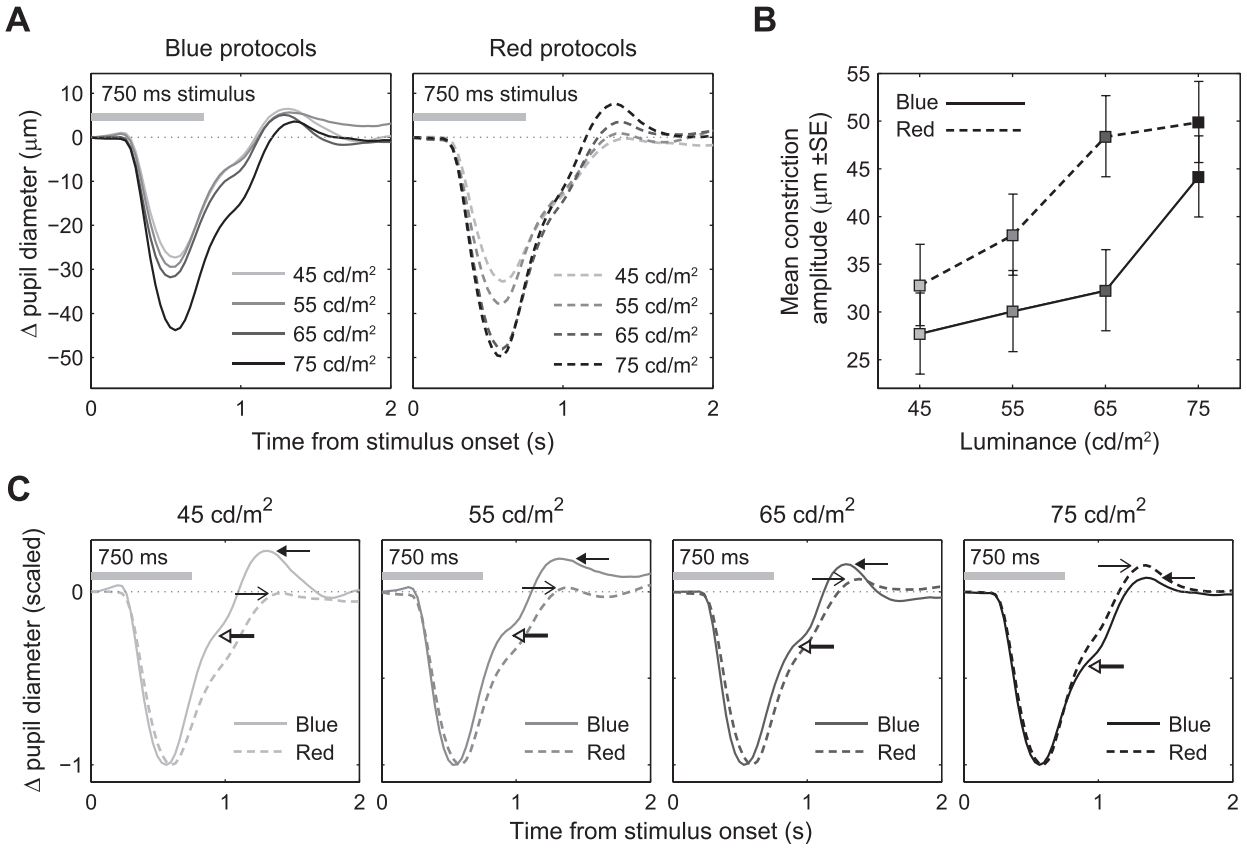

Figure 2. Mean responses from a preliminary experiment comparing red and blue stimulus protocols. (**A**) Average response waveforms for blue and red protocols. (**B**) Mean amplitudes of pupillary responses to blue and red mfPOP protocols were plotted against stimulus luminances (45, 55, 65, or 75 cd/m^2) of each set of protocols. The *red* stimuli produced functions (*dashed lines*) that saturated as luminance increased. In contrast, the blue response waveform (*solid line*) demonstrated increasing gain with stimulus luminance and no evidence of saturation. (**C**) Mean waveforms are scaled as proportions of peak constriction amplitudes. *White headed arrows* indicate the PIPR for each blue protocol: *black-* and *open-headed arrows* show the positive components for red and blue protocols, respectively.

mainly of medium- and long-wavelength light: the M- + L-cone-biased "yellow" protocol, or longer duration 750-ms stimuli consisting mainly of shorter wavelength light: the melanopsin-biased "blue" protocol (see details below). The integration time of melanopsin is long: blue stimuli much shorter than this may exclude the intrinsic response.[25,26] Stimuli in the preliminary experiment had temporal characteristics identical to those of the blue protocol (duration: 750 ms) but used red and blue stimuli presented at four different luminance levels (Table 1).

Each stimulus sequence was separated into segments lasting 30 seconds; the yellow protocol contained 8 of these segments, giving a total recording duration of 4 minutes (Table 1). The blue and red protocols, due to their much longer stimuli and lower presentation rate, consisted of 16 segments with a total recording duration of 8 minutes. Stimuli in all protocols were presented on a photopic background (mean luminance of 10 cd/m^2), the same color as the stimuli. The presence of some spectral components over 500 nm in the blue background should serve to maintain levels of the 11-*cis* melanopsin isomer and enable continuous ipRGC firing.[42] The CIE *x-y* coordinates for yellow protocol test-regions were 0.377 and 0.464, respectively, and 0.408 and 0.515, respectively, for the background (Fig. 1D). This protocol used "partially luminance-balanced" stimuli to minimize the effects of response saturation[12]; therefore, the luminance of test-regions ranged between 67 and 150 cd/m^2, depending on their location in the visual field[10,14] (Fig. 1C). Balancing results in reduced topographic variation in response amplitudes and improves diagnostic power for glaucoma (Maddess T, et al. *IOVS* 2009;50:ARVO E-Abstract 5281). The luminance of all test-regions in the blue protocol was 75 cd/m^2. CIE *x-y* coordinates of these regions were 0.145 and 0.113, respectively, and 0.137 and 0.120, respectively, for the background (Fig. 1E). Luminance-balanced stimuli were not used in this protocol due to finding in the preliminary experiment that response saturation was not present at this level of blue illumination (Fig. 2). Proportional cone activations for the color channels used in both experiments are shown in Figure 3. These were estimated using human cone sensitivity functions[43] and measured spectra at luminances of 75 cd/m^2 for the nuCoria field analyzer red and blue channels and 108 cd/m^2 for yellow.

Response Estimation

Signal processing was carried out using custom-designed software developed using Matlab (release R2010b; MathWorks Inc., Natick, MA, USA). Response waveforms for each test-region were extracted from raw pupillary responses using multiple linear regression as previously described.[6,7,10] This method provided a set of 176 response estimates (waveforms) for each subject and protocol: both direct and consensual responses for left and right eyes for each of the 44 test-regions. Thus, for each region, these response estimates are effectively the mean of the responses to either 60 (yellow protocol) or 15

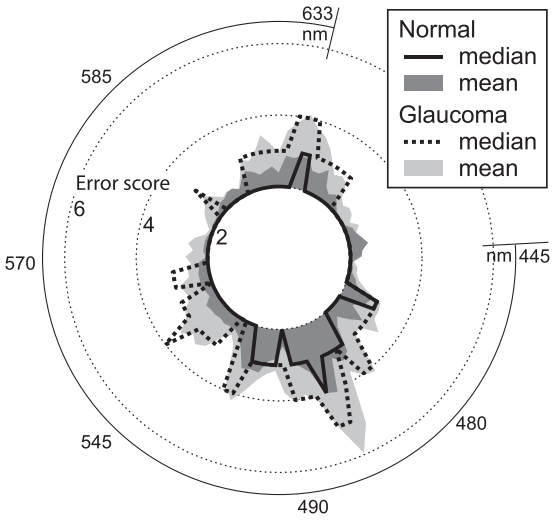

FIGURE 3. Farnsworth 100-hue test (F100) error score characteristics for normal and glaucoma subject groups of the main experiment (for clarity, only the central area of the F100 plots are shown; standard F100 plots extend outwardly to error scores of 14). Median values are represented by *solid* and *dotted black lines* (legend) and mean values by the extent of the *gray shaded areas*. Note the tendency toward *blue-yellow* type III (tritan-like) anomalies in both groups. The scores of glaucoma subjects are significantly higher than those of normal subjects ($P < 0.05$ [see Results, Main Experiment, F100 Color Discrimination]).

(blue protocol) individual stimulus presentations to that region. Pupil diameter measurements were normalized to a mean pupil diameter of 3500 μm as in previous studies, providing constriction amplitudes that are relative to that standard diameter.[9,11,12,19]

Analysis

Sources of variation in the F100 total error scores (TESs) of glaucoma and normal subjects were quantified using multiple linear regression. The effects of relevant study variables on pupillary constriction amplitudes were calculated using a mixed-effects model incorporating restricted maximum likelihood estimation[44] in R software (R Core Team 2013, Vienna, Austria). The distribution of variance in response amplitudes was stabilized initially using a generalized logarithmic transform as described previously[10,18]; model outputs are therefore reported in dB. Random effects were fitted for the nested factors eye within subject, and the remaining variates fitted as fixed effects.

Receiver operating characteristic (ROC) analysis, which offsets the true positive rate of a method against its false positive rate, was used to assess diagnostic performance.[11,19] ROC curves and their area under the curve (AUC) values were calculated for each protocol and severity classification. This involved selecting responses for each test-region from the pupil with the best signal-to-noise ratio (i.e., either the direct or consensual response). *Z*-score deviations from average normal responses were then calculated, incorporating a decibel offset for sex, because mfPOP responses are typically smaller in females.[45] ROC curves were calculated using these *z*-scores for the means of varying-sized subsets of the most deviating test-regions of each eye, from the single worst-performing region (*n*-worst = 1), the mean of the 2 worst-performing regions (*n*-worst = 2), to the mean of all 44 test-region deviations of each field (*n*-worst = 44).

RESULTS

Preliminary Experiment

Mean response waveforms and constriction amplitudes across test-regions, eyes, and subjects are presented in Figure 2. Mean amplitudes of red protocol responses were slightly larger than those of blue (Figs. 2A, 2B). This is most likely due to the larger baseline pupil diameters, and therefore higher retinal illuminance, during testing with red protocols (Fig. 1D; Supplementary Table S2). Constriction amplitudes increased with luminance in both blue and red protocols (Figs. 2A, 2B). Red protocol amplitudes, however, plateaued at 65 cd/m^2 and above; in contrast, blue amplitudes accelerated at equivalent luminances. In blue protocols, this marked increase in amplitude was replicated in the PIPR and also in the decrease of the positive dilation component. There was little evidence of a PIPR in red protocols; the amplitude of the small deflection that was present did not change. In contrast to blue, higher luminance also increased the strength of the positive component. The scaled responses plotted in Figure 2C show that these patterns hold when taken as a proportion of the overall constriction amplitude (Fig. 2C, white-headed arrows indicate the increase in blue PIPR, and black- and open-headed arrows highlight the opposing effects of increased red and blue luminance on the positive response component). In contrast to the responses to red stimuli, the response waveforms and stimulus response function for blue stimuli were consistent with substantial melanopsin involvement.[20,46]

Main Experiment

F100 Color Discrimination. A possible confounding factor for these experiments are color vision deficits from various sources, so color vision was tested in all subjects. F100 TESs ranged from 4 to 169 in normal subjects and from 43 to 169 in patients. Multiple linear regression revealed significant independent effects of both diagnosis and age on color discrimination. The mean TES for normal subjects was 46.5, increasing on average by 16.4 per 10-year increment in age [$t(40) = 2.6$; $P = 0.013$]. Independent of this age effect, patients' scores averaged 33.2 higher than normal subjects [$t(40) = 3.1$, $P = 0.004$]. Mean and median test results for each group are shown in Figure 3, which indicates that the majority of variation in these subjects is due to a tendency toward type III tritan-like anomalies, this being more pronounced in patients.

Pupillary Response Characteristics. Of the 1032 thirty-second protocol segments presented to the subjects in this study's main experiment, only 4 segments needed to be repeated due to the criterion lack of more than 15% of that segment's data. The mean pupillary constriction waveforms for the two protocols differed slightly; the time course of constrictions elicited by the blue protocol was substantially longer, with evidence of a PIPR sustained component following the peak of the response (Fig. 4A).

Pupillary response characteristics were assessed by stimulus protocol, diagnostic status, age, sex, color discrimination, and location of the test-region in the visual field. The yellow protocol produced mean constriction amplitudes that were significantly smaller than those of the blue ($16.26 - 11.64 = 4.62$ dB; $t(7481) = -104.3$; $P < 0.0001$) (Table 2). Mean baseline pupil diameters differed in a manner similar to those in the preliminary experiment, with the longer wavelength yellow protocol producing a larger diameter of 3.47 mm than that of blue at 2.70 mm. The smaller responses obtained using this yellow protocol are therefore most likely due to the short

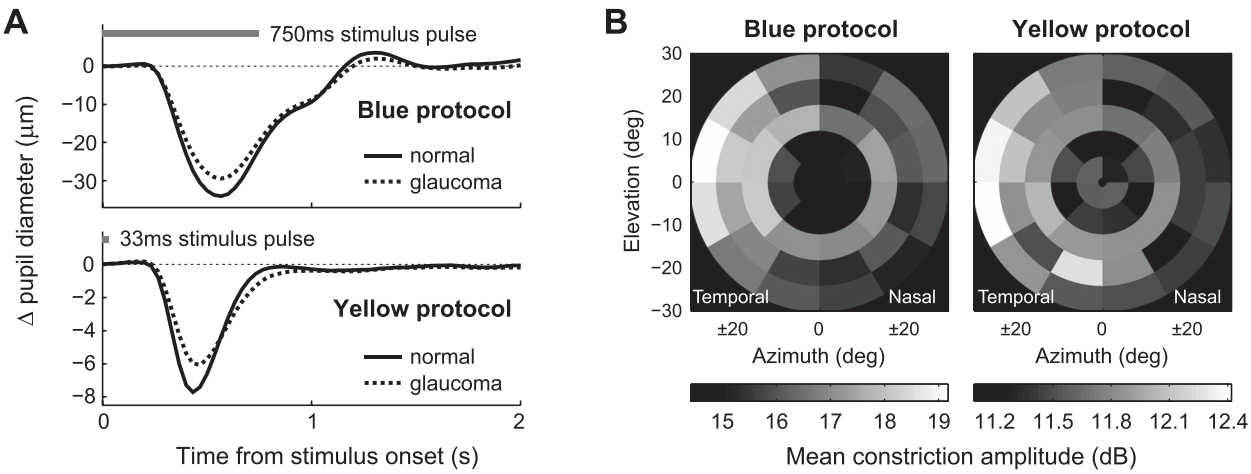

Figure 4. **(A)** Averaged pupillary response waveforms showing the general form taken by responses to the two different stimulus protocols of the main experiment (means for glaucoma and normal subjects computed across eyes, pupils, and visual field regions). The *blue* response waveforms show a PIPR component in the redilation phase. **(B)** Constriction amplitude means by region from a mixed-effects model incorporating effects for sex, eye, age, F100 TES, and diagnosis of subjects. Thus, these regional means represent the responses of left eyes of male subjects aged 60 with normal vision and average color sensitivity, and are subject to modification by the effects reported in Table 2. All results are mapped as left-eye–equivalent visual fields with the temporal field shown here on the *left*. Constriction amplitudes were largest in the temporal field in both blue and yellow protocols.

duration of the yellow stimuli. In both yellow and blue protocols, the largest regional constriction amplitudes were obtained to stimuli in the temporal field (Fig. 4B). Mean constriction amplitudes of eyes with moderate to severe glaucoma were significantly smaller than those of normal subjects in both protocols: blue by −1.32 dB [$t(40) = -2.29$; $P = 0.027$], yellow by a smaller but more significant margin of −0.93 dB [$t(40) = -3.13$; $P = 0.003$] (Table 2). No significant difference was observed between mild glaucoma and normal subjects or for any other of the fitted variates.

Diagnostic Accuracy. ROC plots for the *n*-worst test-regions that produced the highest AUC for each severity are shown in Figure 5A. The diagnostic performance of the two protocols was quite similar (Table 3). On inclusion of all subject eyes (i.e., all severities) in the analysis, an overall AUC value of 70.9% (±5.6% SE, *n*-worst = 41) was obtained using the blue protocol, and 71.3% (±5.9% SE, *n*-worst = 1) using the yellow protocol. Both of the protocols were able to detect eyes classified as severe (HFA MD less than −12 dB) with 100% accuracy, and both produced AUCs of 79% for eyes classified as moderate.

The two protocols differed, however, in the pattern of which *n*-worst regions produced the highest AUCs. In moderate to severe eyes, the accuracy of the yellow protocol was highest when only each subject's single most deviating test-regions were included in the analysis. The blue protocol, however, demonstrated increasing accuracy on inclusion of larger numbers of these worst performing regions (Fig. 5B). Thus, this protocol appeared to have lesser capacity than yellow to detect localized damage in advanced disease, relying instead on measures akin to the mean defect to derive diagnostic power. In contrast, in eyes classified as mild, both of the protocols were most accurate using just the single worst-performing region. The blue protocol produced a slightly higher AUC, but this value was not significantly different from that produced by the yellow protocol.

Discussion

The potential of mfPOP as an emerging diagnostic tool for glaucoma is considerable, with its diagnostic accuracy comparable to commonly used forms of perimetry.[9,19] This study

Table 2. Fixed Effects of Study Variables From Linear Mixed-Effects Models for Blue and Yellow mfPOP Protocols

	Blue Protocol				Yellow Protocol			
	***b*, dB**	***df***	***t***	***P***	***b*, dB**	***df***	***t***	***P***
Constant	16.259	3698	–	–	11.639	3698	–	–
DecadeRel60	0.157	39	0.55	0.5823	0.132	39	1.01	0.3175
Right eye	−0.059	40	−0.41	0.6871	−0.031	40	−0.26	0.7933
Female	−0.164	39	−0.37	0.7153	−0.211	39	−1.02	0.3140
Glaucoma, mild/ND*	0.005	40	0.01	0.9919	−0.221	40	−0.89	0.3793
Glaucoma, moderate/severe	−1.318	40	−2.29	0.0272	−0.925	40	−3.13	0.0033
F100	−0.021	39	−0.31	0.7590	0.056	39	1.80	0.0793

Additive effects (*b*) are relative to the *y* intercept or *Constant*, which describes the mean of constriction amplitudes across the 44 test-regions of left eyes of male subjects aged 60 with normal vision and average color sensitivity. DecadeRel60 refers to an additive slope in dB/decade relative to 60 years. For the variable F100, 120 (the normative mean TES for a 60-year-old subject[37]) was subtracted from subjects' total error scores in order to maintain parity with DecadeRel60. The result was then divided by 10 to provide a more practical measure; therefore, the fitted values refer to the additive effect of F100 increments of 10, relative to a TES of 120 on constriction amplitudes.

* Putatively normal eyes of glaucoma patients.

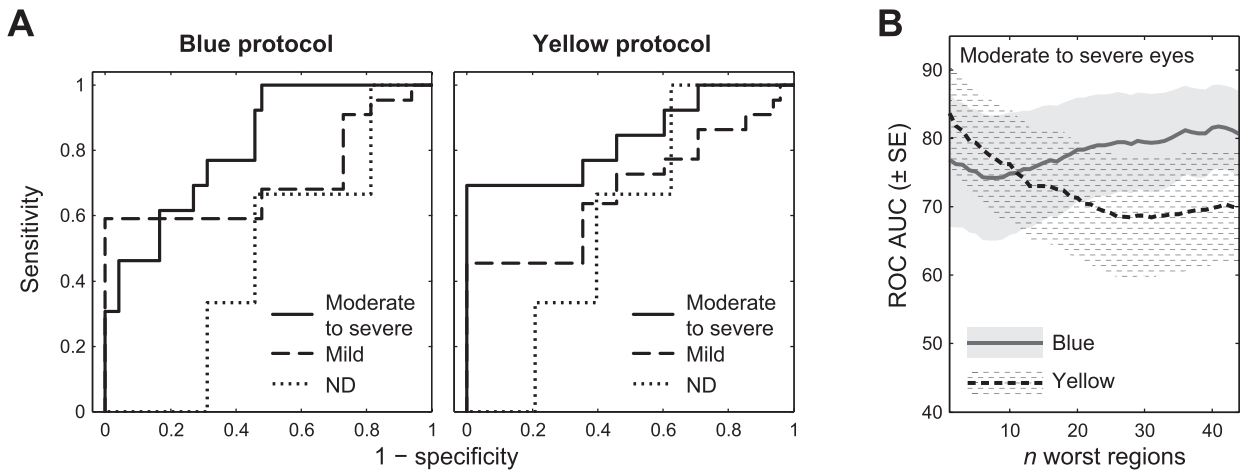

Figure 5. (**A**) ROC curves for each level of functional defect for blue and yellow protocols (ND = putatively normal eyes of glaucoma subjects). Precise AUC values, SE and *n*-worst values are reported in Table 3. (**B**) Estimation of ROC AUC values was carried out using varying numbers of the regions having the greatest deviations from normal, described as *n*-worst. This plot shows the AUC values obtained using *n*-worst visual field deviations ranging from $n = 1$ to 44 for both protocols, for the 13 eyes classified as moderate to severe. The yellow protocol achieved its highest accuracy using only very few of these worst performing regions. The blue protocol, in contrast, improved in accuracy as more regions were included in the analysis. This pattern reflects the overall trend for the blue and yellow protocols. Notice also that the AUC values for what is essentially the mean defect (*n*-worst = 44) also differ for blue and yellow stimuli.

aimed to determine whether improvements could be made to methods currently being developed by targeting the intrinsic component of the ipRGC response. Pupil perimetry using single blue stimuli have been undertaken[47,48]; however, these studies used dark-adapted subjects, so responses will have also involved rod photoreceptors. The use of a photopic blue adapting background in this experiment aimed to minimize rod involvement and facilitate the observation of melanopsin responses.

Preliminary Experiment and Melanopsin Involvement

As well as being largely responsible for the PIPR, some results suggest that melanopsin has a substantial influence on early response components at luminance levels and durations similar to those used in our main experiment (Fig. 1).[20] Additionally, at pupillary diameters equivalent to those achieved using blue mfPOP (Supplementary Table S2), the spectral sensitivity of these early response components appears to be dominated by melanopsin.[26] Therefore, the potential to obtain melanopsin-influenced mfPOP responses exists; several characteristics of the responses obtained to blue stimulation in these experiments appear to confirm this.

The accelerating stimulus-response function shown in Figure 2B and the differences between red and blue later response components (Figs. 2A, 2C) are consistent with observations of the progressive domination of pupil responses by melanopsin at higher luminances.[26] This contrasts with the saturating stimulus-response functions we obtained previously using yellow stimuli[12] and which were also observed using red stimuli in the preliminary experiment (Fig. 2B). The decrease in the positive component of blue responses is consistent with the greatly reduced β-wave seen in isolated melanopsin responses to flash electroretinography in macaques[20] and lends strength to the assertion that melanopsin is involved in these responses to 750-ms blue mfPOP stimuli. The congruence between the changes in peak amplitude of constrictions and both the PIPR and positive dilation component is highly suggestive of a substantial melanopsin contribution to early (i.e., response amplitudes), as well as later components. It seems reasonable therefore to conclude that, although cone photoreceptors have undoubtedly participated in responses to the blue protocol of the main experiment as sources of both excitatory and inhibitory input (Fig. 3, cone activations), pupil constriction amplitudes in the blue protocol were also substantially influenced by melanopsin.

Short-Wavelength Discrimination

Normal aging results in increases in absorption of shorter wavelength light by the crystalline lens, observable as

Table 3. Percent ROC Area Under the Curve (AUC) and AUC Standard Error (SE) Values

	Blue Protocol			Yellow Protocol		
Severity (*n* eyes)	**AUC, %**	**SE, %**	***n*-worst**	**AUC, %**	**SE, %**	***n*-worst**
Moderate to severe (13)	81.7	6.1	42	83.7	7.4	1
Mild (22)	71.1	8.0	1	67.7	7.7	1
ND* (3)	47.2	13.4	44	59.0	11.5	37:38

ROC estimates were obtained using response amplitudes and the optimal number of *n*-worst deviations from normal from any position in the visual field. Diagnostic accuracy using the yellow protocol was high when only a limited number of the worst performing regions were included in the analysis (Fig. 5B). The blue protocol, however, displayed a tendency for accuracy to increase with the inclusion of more regions. This was particularly apparent for eyes with moderate to severe defects.

* Putatively normal eyes of glaucoma patients.

yellowing or brunescence,[30–33] as well as changes in the function of S-cone pathways.[49] Evidence of this is seen in the increase in F100 TESs with age and the reduced blue-yellow discrimination illustrated in Figure 3. The antagonistic effect of S-cone stimulation on the intrinsic and M- + L-cone–derived ipRGC response is postulated to arise in DB6 bipolar cells, the major source of synaptic input to ipRGCs.[50] This is proposed to be due to S-cone ON inactivation of ionotropic glutamatergic ion channels, preferentially expressed at S-cone synapses, leading to hyperpolarization of the DB6 cell. This would counteract the depolarization caused by the M- + L-cone inactivation of metabotropic ion channels in these same cells and reduce excitatory input to ipRGCs.[51] The potential effect of brunescence on ipRGC responses is therefore twofold: (1) an overall reduction in the intrinsic melanopsin response; and (2) an increased bipolar cell synaptic input due to a reduction in antagonistic signal arising in S-cones. No significant independent effect of age or color sensitivity was observed in responses to the blue protocol (Table 2). A possible explanation for this is that any effects of brunescence may have counteracted each other (i.e., reduced melanopsin responses balanced by reduced S-cone antagonism). Similarly, age was not seen to significantly affect responses to the yellow protocol (Table 2), perhaps spared by the longer wavelengths of the stimuli. The alternative explanation, that brunescence did not affect retinal function, is unlikely because age was shown to have a significant effect on F100 error scores.

Abnormalities in blue-yellow discrimination also occur in glaucoma, independent of the effects of aging or media opacities,[52–55] and probably account for the greater type III color anomalies seen in patients (Fig. 4). This has been attributed to selective RGC loss[52]; however, pressure-related damage to S-cone bipolar cells has also been implicated.[56] Reduced S-cone inhibitory input could potentially mask the effects of RGC loss on pupillary constrictions by increasing responses in the remaining functioning RGCs. This may account for the greater variability in patients' response amplitudes to the blue protocol (Table 2).

Identification of Localized Dysfunction

The restriction of comparisons between normal and glaucoma subjects to different sized subsets of *n*-worst regions can be used as a measure of a test's ability to identify localized areas of dysfunction. Although much damage to retinal ganglion cells in glaucoma is diffuse,[57,58] localized scotomas are an obvious feature. In severe eyes, reliance of the blue protocol on mean deviations to achieve best diagnostic accuracy contrasts with the yellow protocol, where the best results were obtained using only the few worst performing test-regions, highlighting its ability to detect highly diagnostic localized depressions in sensitivity (Fig. 5B). Considering only the mean defect (i.e., *n*-worst = 44), diagnostic performance was quite different for yellow and blue stimuli. If these protocols' diagnostic accuracies were comparable, they would be expected to produce similar mean defect–related ROC values. This is clearly not the case. Taken together, the larger mean reduction in regional amplitudes for yellow and the very different response patterns of the two protocols in eyes with established scotomas (Fig. 5B) suggest that different physiology and possibly even different neural pathways are involved.

Postreceptor retinal factors, such as differently sized RGC receptive fields, are most likely not responsible; cone-mediated receptive fields of ipRGCs are colocalized with their dendritic arborization,[21] and blue-yellow RGC receptive fields in primates, although slightly larger than those of red-green sensitive RGCs,[59] are not different enough to account for this. Forward scatter of light transmitted by the aging crystalline lens, although more prevalent at shorter wavelengths,[33,60,61] is not likely to result in sufficient blurring of stimuli to render scotomas invisible.[60,62] Cortical input to the pupillary pathway could potentially play a role,[36] perhaps using a similar global mechanism to the accommodative response to optical defocus,[63,64] although exactly how this would result in these differences between blue and yellow is not clear.

Conclusions

This study's aim was to determine the viability of mfPOP stimuli that target the intrinsic melanopsin response of ipRGCs. Little difference was observed between the overall diagnostic accuracies of the blue and yellow stimuli, the slightly higher ROC AUC of the blue protocol not being significantly different from yellow. The blue protocol produced much larger constriction amplitudes and signal-to-noise ratios than the yellow protocol, without evidence of response saturation. Yellow stimuli produced less variable reductions in patients' response amplitudes and had better sensitivity to localized defects in established disease. In advanced disease, the diagnostic value of the blue protocol appeared somewhat prone to confounding factors related to aging and the disease process; similar issues have previously been found to hamper short-wavelength automated perimetry.[65,66] Although this melanopsin-targeted protocol did not appear to lend any advantage in identification of later-stage glaucoma, it may have potential in the detection and management of early disease or possibly in other diseases in which sensitivity to short-wavelength light is affected. The replication of this study using a larger cohort would likely clarify the potential benefits of blue mfPOP stimuli relative to those of yellow in early glaucoma.

Acknowledgments

Supported by the Australian Research Council (ARC) through the ARC Centre of Excellence in Vision Science (CE0561903).

Disclosure: **C.F. Carle**, NuCoria (I) P; **A.C. James**, NuCoria (I), P; **M. Kolic**, Seeing Machines (E); **R.W. Essex**, None; **T. Maddess**, NuCoria (I), P

References

1. Kardon RH, Kirkali PA, Thompson HS. Automated pupil perimetry. Pupil field mapping in patients and normal subjects. *Ophthalmology*. 1991;98:485–495.
2. Schmid R, Luedtke H, Wilhelm BJ, Wilhelm H. Pupil campimetry in patients with visual field loss. *Eur J Neurol*. 2005;12:602–608.
3. Fankhauser F II, Flammer J. Puptrak 1.0–a new semiautomated system for pupillometry with the Octopus perimeter: a preliminary report. *Doc Ophthalmol*. 1989;73:235–248.
4. Wilhelm H, Neitzel J, Wilhelm B, et al. Pupil perimetry using M-sequence stimulation technique. *Invest Ophthalmol Vis Sci*. 2000;41:1229–1238.
5. Tan L, Kondo M, Sato M, Kondo N, Miyake Y. Multifocal pupillary light response fields in normal subjects and patients with visual field defects. *Vision Res*. 2001;41:1073–1084.
6. James AC. The pattern-pulse multifocal visual evoked potential. *Invest Ophthalmol Vis Sci*. 2003;44:879–890.
7. James AC, Ruseckaite R, Maddess T. Effect of temporal sparseness and dichoptic presentation on multifocal visual evoked potentials. *Vis Neurosci*. 2005;22:45–54.
8. Ruseckaite R, Maddess T, Danta G, Lueck CJ, James AC. Sparse multifocal stimuli for the detection of multiple sclerosis. *Ann Neurol*. 2005;57:904–913.

9. Carle CF, James AC, Kolic M, Loh YW, Maddess T. High-resolution multifocal pupillographic objective perimetry in glaucoma. *Invest Ophthalmol Vis Sci*. 2011;52:604–610.
10. Carle CF, James AC, Kolic M, Essex RW, Maddess T. Luminance and colour variant pupil perimetry in glaucoma. *Clin Exp Ophthalmol*. 2014;42:815–824.
11. Bell A, James AC, Kolic M, Essex RW, Maddess T. Dichoptic multifocal pupillography reveals afferent visual field defects in early type 2 diabetes. *Invest Ophthalmol Vis Sci*. 2010;51:602–608.
12. Maddess T, Ho YL, Wong SS, et al. Multifocal pupillographic perimetry with white and colored stimuli. *J Glaucoma*. 2011;20:336–343.
13. Sabeti F, Maddess T, Essex RW, James AC. Multifocal pupillographic assessment of age-related macular degeneration. *Optom Vis Sci*. 2011;88:1477–1485.
14. Sabeti F, James AC, Essex RW, Maddess T. Multifocal pupillography identifies retinal dysfunction in early age-related macular degeneration. *Graefes Arch Clin Exp Ophthalmol*. 2013;251:1707–1716.
15. Sabeti F, Maddess T, Essex RW, Saikal A, James A, Carle C. Multifocal pupillography in early age-related macular degeneration. *Optom Vis Sci*. 2014;91:904–915.
16. Sabeti F, Maddess T, Essex RW, James AC. Multifocal pupillography identifies ranibizumab-induced changes in retinal function for exudative age-related macular degeneration. *Invest Ophthalmol Vis Sci*. 2012;53:253–260.
17. Carle CF, Maddess T, James AC. Contraction anisocoria: segregation, summation, and saturation in the pupillary pathway. *Invest Ophthalmol Vis Sci*. 2011;52:2365–2371.
18. Carle CF, James AC, Maddess T. The pupillary response to color and luminance variant multifocal stimuli. *Invest Ophthalmol Vis Sci*. 2013;54:467–475.
19. Maddess T, Bedford SM, Goh XL, James AC. Multifocal pupillographic visual field testing in glaucoma. *Clin Exp Ophthalmol*. 2009;37:678–686.
20. Gamlin PD, McDougal DH, Pokorny J, Smith VC, Yau KW, Dacey DM. Human and macaque pupil responses driven by melanopsin-containing retinal ganglion cells. *Vision Res*. 2007;47:946–954.
21. Dacey DM, Liao HW, Peterson BB, et al. Melanopsin-expressing ganglion cells in primate retina signal colour and irradiance and project to the LGN. *Nature*. 2005;433:749–754.
22. Melyan Z, Tarttelin EE, Bellingham J, Lucas RJ, Hankins MW. Addition of human melanopsin renders mammalian cells photoresponsive. *Nature*. 2005;433:741–745.
23. Qiu X, Kumbalasiri T, Carlson SM, et al. Induction of photosensitivity by heterologous expression of melanopsin. *Nature*. 2005;433:745–749.
24. Fu Y, Liao HW, Do MT, Yau KW. Non-image-forming ocular photoreception in vertebrates. *Curr Opin Neurobiol*. 2005;15:415–422.
25. Kardon R, Anderson SC, Damarjian TG, Grace EM, Stone E, Kawasaki A. Chromatic pupil responses: preferential activation of the melanopsin-mediated versus outer photoreceptor-mediated pupil light reflex. *Ophthalmology*. 2009;116:1564–1573.
26. McDougal DH, Gamlin PD. The influence of intrinsically-photosensitive retinal ganglion cells on the spectral sensitivity and response dynamics of the human pupillary light reflex. *Vision Res*. 2010;50:72–87.
27. Park JC, Moura AL, Raza AS, Rhee DW, Kardon RH, Hood DC. Toward a clinical protocol for assessing rod, cone and melanopsin contributions to the human pupil response. *Invest Ophthalmol Vis Sci*. 2011;52:6624–6635.
28. Feigl B, Mattes D, Thomas R, Zele AJ. Intrinsically photosensitive (melanopsin) retinal ganglion cell function in glaucoma. *Invest Ophthalmol Vis Sci*. 2011;52:4362–4367.
29. Kankipati L, Girkin CA, Gamlin PD. The post-illumination pupil response is reduced in glaucoma patients. *Invest Ophthalmol Vis Sci*. 2011;52:2287–2292.
30. Pokorny J, Smith VC, Lutze M. Aging of the human lens. *Appl Opt*. 1987;26:1437–1440.
31. Fortune B, Johnson CA. Decline of photopic multifocal electroretinogram responses with age is due primarily to preretinal optical factors. *J Opt Soc Am A Opt Image Sci Vis*. 2002;19:173–184.
32. Sample PA, Esterson FD, Weinreb RN, Boynton RM. The aging lens - in vivo assessment of light-absorption in 84 human eyes. *Invest Ophthalmol Vis Sci*. 1988;29:1306–1311.
33. van de Kraats J, van Norren D. Optical density of the aging human ocular media in the visible and the UV. *J Opt Soc Am A Opt Image Sci Vis*. 2007;24:1842–1857.
34. Chen SF, Chang Y, Wu JC. The spatial distribution of macular pigment in humans. *Cur Eye Res*. 2001;23:422–434.
35. Zagers NP, van Norren D. Absorption of the eye lens and macular pigment derived from the reflectance of cone photoreceptors. *J Opt Soc Am A Opt Image Sci Vis*. 2004;21:2257–2268.
36. Gamlin PD. The pretectum: connections and oculomotor-related roles. *Prog Brain Res*. 2006;151:379–405.
37. Drew P, Sayres R, Watanabe K, Shimojo S. Pupillary response to chromatic flicker. *Exp Brain Res*. 2001;136:256–262.
38. Varjú D. Human pupil dynamics. In: Reichardt W, ed. *Proceedings of the International School of Physics "Enrico Fermi," Course XLIII*. New York: Academic; 1969:442–464.
39. Jusuf PR, Lee SC, Hannibal J, Grunert U. Characterization and synaptic connectivity of melanopsin-containing ganglion cells in the primate retina. *Eur J Neurosci*. 2007;26:2906–2921.
40. Kinnear PR, Sahraie A. New Farnsworth-Munsell 100 hue test norms of normal observers for each year of age 5–22 and for age decades 30–70. *Br J Ophthalmol*. 2002;86:1408–1411.
41. Anderson AJ, Johnson CA. Frequency-doubling technology perimetry and optical defocus. *Invest Ophthalmol Vis Sci*. 2003;44:4147–4152.
42. Mure LS, Cornut PL, Rieux C, et al. Melanopsin bistability: a fly's eye technology in the human retina. *PLoS One*. 2009;4:-.
43. Stockman A, MacLeod DI, Johnson NE. Spectral sensitivities of the human cones. *J Opt Soc Am A Opt Image Sci Vis*. 1993;10:2491–2521.
44. Bates DM. Computational methods for mixed models. In: *LME4: Mixed-Effects Modeling with R*. New York: Springer Publishing; 2010:99–118.
45. Maddess T, Essex RW, Kolic M, Carle CF, James AC. High versus low density multifocal pupillographic objective perimetry in glaucoma. *Clin Exp Ophthalmol*. 2013;41:140–147.
46. Lei S, Goltz HC, Chandrakumar M, Wong AMF. Full-field chromatic pupillometry for the assessment of the postillumination pupil response driven by melanopsin-containing retinal ganglion cells. *Invest Ophthalmol Vis Sci*. 2014;55:4496–4503.
47. Tatham AJ, Meira-Freitas D, Weinreb RN, Zangwill LM, Medeiros FA. Detecting glaucoma using automated pupillography. *Ophthalmology*. 2014;121:1185–1193.
48. Skaat A, Sher I, Kolker A, et al. Pupillometer-based objective chromatic perimetry in normal eyes and patients with retinal photoreceptor dystrophies. *Invest Ophthalmol Vis Sci*. 2013;54:2761–2770.
49. Suzuki S, Horiguchi M, Tanikawa A, Miyake Y, Kondo M. Effect of age on short-wavelength sensitive cone electroretinogram and long and middle-wavelength sensitive cone electroretinogram. *Jpn J Ophthalmol*. 1998;42:424–430.
50. Grunert U, Jusuf PR, Lee SC, Nguyen DT. Bipolar input to melanopsin containing ganglion cells in primate retina. *Vis Neurosci*. 2010;28:1–12.

Investigative Ophthalmology & Visual Science

51. Dacey DM, Crook JD, Packer OS. Distinct synaptic mechanisms create parallel S-ON and S-OFF color opponent pathways in the primate retina. *Vis Neurosci*. 2014;31:139–151.
52. Pacheco-Cutillas M, Sahraie A, Edgar DF. Acquired colour vision defects in glaucoma - their detection and clinical significance. *Br J Ophthalmol*. 1999;83:1396–1402.
53. Drance SM, Lakowski R, Schulzer M, Douglas GR. Acquired color-vision changes in glaucoma—use of 100-hue test and Pickford anomaloscope as predictors of glaucomatous field change. *Arch Ophthalmol*. 1981;99:829–831.
54. Sample PA, Boynton RM, Weinreb RN. Isolating the color-vision loss in primary open-angle glaucoma. *Am J Ophthalmol*. 1988;106:686–691.
55. Gray LS, Heron G, Cassidy D, et al. Comparison of age-related changes in short-wavelength-sensitive cone thresholds between normals and patients with primary open-angle glaucoma. *Optom Vis Sci*. 1995;72:205–209.
56. Drasdo N, Aldebasi YH, Chiti Z, Mortlock KE, Morgan JE, North RV. The S-cone PhNR and pattern ERG in primary open angle glaucoma. *Invest Ophthalmol Vis Sci*. 2001;42:1266–1272.
57. Henson DB, Artes PH, Chauhan BC. Diffuse loss of sensitivity in early glaucoma. *Invest Ophthalmol Vis Sci*. 1999;40:3147–3151.
58. Chauhan BC, LeBlanc RP, Shaw AM, Chan AB, McCormick TA. Repeatable diffuse visual field loss in open-angle glaucoma. *Ophthalmology*. 1997;104:532–538.
59. Solomon SG, Lee BB, White AJ, Ruttiger L, Martin PR. Chromatic organization of ganglion cell receptive fields in the peripheral retina. *J Neurosci*. 2005;25:4527–4539.
60. Van den Berg TJ, Ijspeert JK. Light scattering in donor lenses. *Vision Res*. 1995;35:169–177.
61. Thaung J, Sjostrand J. Integrated light scattering as a function of wavelength in donor lenses. *J Opt Soc Am A Opt Image Sci Vis*. 2002;19:152–157.
62. Artal P, Ferro M, Miranda I, Navarro R. Effects of aging in retinal image quality. *J Opt Soc Am A Opt Image Sci Vis*. 1993;10:1656–1662.
63. Slooter J. Clinical use of visual-acuity measured with pupil responses. *Documenta Ophthalmologica*. 1981;50:389–399.
64. Phillips S, Stark L. Blur—sufficient accommodative stimulus. *Documenta Ophthalmologica*. 1977;43:65–89.
65. Gardiner SK, Johnson CA, Spry PG. Normal age-related sensitivity loss for a variety of visual functions throughout the visual field. *Optom Vis Sci*. 2006;83:438–443.
66. Anderson RS, Redmond T, McDowell DR, Breslin KMM, Zlatkova MB. The robustness of various forms of perimetry to different levels of induced intraocular stray light. *Invest Ophthalmol Vis Sci*. 2009;50:4022–4028.

Investigative Ophthalmology & Visual Science